



HAL
open science

Fluorescent Labeling and 2-Photon Imaging of Mouse Tooth Pulp Nociceptors

Aklesso Kadala, P. Sotelo-Hitschfeld, Z. Ahmad, P. Tripal, B. Schmid, A.
Mueller, L. Bernal, Z. Winter, S. Brauchi, U. Lohbauer, et al.

► **To cite this version:**

Aklesso Kadala, P. Sotelo-Hitschfeld, Z. Ahmad, P. Tripal, B. Schmid, et al.. Fluorescent Labeling and 2-Photon Imaging of Mouse Tooth Pulp Nociceptors. *Journal of Dental Research*, 2018, 97 (4), pp.460-466. 10.1177/0022034517740577 . hal-03404337

HAL Id: hal-03404337

<https://hal.science/hal-03404337v1>

Submitted on 21 Dec 2023

HAL is a multi-disciplinary open access archive for the deposit and dissemination of scientific research documents, whether they are published or not. The documents may come from teaching and research institutions in France or abroad, or from public or private research centers.

L'archive ouverte pluridisciplinaire **HAL**, est destinée au dépôt et à la diffusion de documents scientifiques de niveau recherche, publiés ou non, émanant des établissements d'enseignement et de recherche français ou étrangers, des laboratoires publics ou privés.



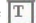

Distributed under a Creative Commons Attribution - NonCommercial 4.0 International License

Page Proof Instructions and Queries

Journal Title: Journal of Dental Research

Article Number: 740577

Thank you for choosing to publish with us. This is your final opportunity to ensure your article will be accurate at publication. Please review your proof carefully and respond to the queries using the circled tools in the image below, which are available by clicking **“Comment”** from the right-side menu in Adobe Reader DC.*

Please use *only* the tools circled in the image, as edits via other tools/methods can be lost during file conversion. For comments, questions, or formatting requests, please use . Please do *not* use comment bubbles/sticky notes .



*If you do not see these tools, please ensure you have opened this file with **Adobe Reader DC**, available for free at get.adobe.com/reader or by going to Help > Check for Updates within other versions of Reader. For more detailed instructions, please see us.sagepub.com/ReaderXProofs.

No.	Query
1	Please check that all authors are listed in the proper order; clarify which part of each author’s name is his or her surname; and verify that all author names are correctly spelled/punctuated and are presented in a manner consistent with any prior publications.
2	Please review the entire document for typographical errors, mathematical errors, and any other necessary corrections; check headings, tables, and figures.
3	Please confirm that you have sufficiently reviewed your proof and queries, and that you understand this is your FINAL opportunity to review your article before publication.
4	Please ensure all abbreviations are presented consistently.
5	Please review “Using” sentence for edit.
6	No more than six key words should be included selected from Medical Subject Headings (MeSH) to be used for indexing of articles. See: http://www.nlm.nih.gov/mesh/MBrowser.html for information on the selection of key words. Words that are contained in the article title must not be included as key words.
7	Check text for minor clarification: “when applied to locally restricted sites of innervation”?
8	Please review “Fluorophores” sentence for minor edits—note particularly that “Dil” has been updated to “Dil” 2 times (is that correct?).
9	Please confirm Figure 2A citation order.
10	Please confirm this statement.

Fluorescent Labeling and 2-Photon Imaging of Mouse Tooth Pulp Nociceptors

Journal of Dental Research
1–7
© International & American Associations
for Dental Research 2017
Reprints and permissions:
sagepub.com/journalsPermissions.nav
DOI: 10.1177/0022034517740577
journals.sagepub.com/home/jdr

A. Kadala^{1*}, P. Sotelo-Hitschfeld^{1,2*}, Z. Ahmad¹, P. Tripal³, B. Schmid³,
A. Mueller¹, L. Bernal¹, Z. Winter¹, S. Brauchi², U. Lohbauer⁴, K. Messlinger⁵,
J.K. Lennerz⁶, and K. Zimmermann¹ [AQ: 1][AQ: 2][AQ: 3][AQ: 4]

Abstract

Retrograde fluorescent labeling of dental primary afferent neurons (DPANs) has been described in rats through crystalline fluorescent Dil, while in the mouse, this technique was yet achieved with only Fluoro-Gold, a neurotoxic fluorescent dye with membrane penetration characteristics superior to the carbocyanine dyes. We reevaluated this technique in the rat with the aim to transfer it to the mouse because comprehensive physiologic studies require access to the mouse as model organism. Using conventional immunohistochemistry, we assessed in rats and mice the speed of axonal dye transport from the application site to the trigeminal ganglion, the numbers of stained DPANs, and the fluorescence intensity via 1) conventional crystalline Dil and 2) a novel Dil formulation with improved penetration properties and staining efficiency. [AQ: 5] A 3-dimensional reconstruction of an entire trigeminal ganglion with 2-photon laser scanning fluorescence microscopy permitted visualization of DPANs in all 3 divisions of the trigeminal nerve. We quantified DPANs in mice expressing the farnesylated enhanced green fluorescent protein (EGFPf) from the transient receptor potential cation channel subfamily M member 8 (TRPM8^{EGFPf/+}) locus in the 3 branches. We also evaluated the viability of the labeled DPANs in dissociated trigeminal ganglion cultures using calcium microfluorometry, and we assessed the sensitivity to capsaicin, an agonist of the TRPV1 receptor. Reproducible Dil labeling of DPANs in the mouse is an important tool 1) to investigate the molecular and functional specialization of DPANs within the trigeminal nociceptive system and 2) to recognize exclusive molecular characteristics that differentiate nociception in the trigeminal system from that in the somatic system. A versatile tool to enhance our understanding of the molecular composition and characteristics of DPANs will be essential for the development of mechanism-based therapeutic approaches for dentine hypersensitivity and inflammatory tooth pain.

Keywords: dental pulp, TRPM8, TRPV1, dental primary afferent, trigeminal ganglion, carbocyanine dye, Fluoro Gold [AQ: 6]

Introduction

Recent RNA sequencing efforts have revealed substantial diversity of functionally distinct neuron subtypes in the primary sensory system. Based on their unique transcriptional fingerprint, 11 types can be distinguished and serve mechanoreception, proprioception, thermosensation, itch, and nociception (Usoskin et al. 2015). Briefly, via single-cell sampling in combination with sequencing and grouping of related expression profiles, cell types can be classified in an unbiased fashion. The resulting catalog of somatic sensation unveiled a previously unknown level of complexity devoid of morphologic and functional information. Linking sensory subtype classification to functional and organ-specific information can be achieved only by direct and unambiguous labeling of neuronal subpopulations. This goal is commonly achieved by retrograde labeling with lipophilic carbocyanine dyes, which label sensory neuron cell bodies by retrograde transport when applied locally restricted [AQ: 7] to sites of innervation. The dye intercalates into nerve terminal membranes or at sites of axonal discontinuation; it is transported to the soma by axoplasmic transport; and it does not measurably interfere with cell viability and physiologic parameters (Honig and Hume

¹Klinik für Anästhesiologie, Universitätsklinikum Erlangen, Friedrich-Alexander Universität Erlangen-Nürnberg, Erlangen, Germany

²Instituto de Fisiología, Facultad de Medicina, Escuela de Graduados, Facultad de Ciencias, Universidad Austral de Chile, Valdivia, Chile

³Optical Imaging Centre Erlangen, Friedrich-Alexander Universität Erlangen-Nürnberg, Erlangen, Germany

⁴Klinik für Zahnerhaltung und Parodontologie, Universitätsklinikum Erlangen, Friedrich-Alexander Universität Erlangen-Nürnberg, Erlangen, Germany

⁵Institut für Physiologie und Pathophysiologie, Friedrich-Alexander Universität Erlangen-Nürnberg, Erlangen, Germany

⁶Center for Integrated Diagnostics, Massachusetts General Hospital, Harvard Medical School, Boston, USA

*Authors contributing equally to this article.

A supplemental appendix to this article is available online.

Corresponding Authors:

K. Zimmermann, Universitätsklinikum Erlangen, Friedrich-Alexander Universität Erlangen-Nürnberg Klinik für Anästhesiologie, Krankenhausstraße 12, 91054 Erlangen, Germany.

Email: katharina.zimmermann@fau.de

J.K. Lennerz, Center for Integrated Diagnostics, Department of Pathology, Massachusetts General Hospital, Harvard Medical School, 55 Fruit Street, Boston, MA 02114, USA.

Email: jlennerz@partners.org

1986, 1989). In contrast to Fluoro-Gold (FG), carbocyanine dyes allow long-term staining of tissue (Honig and Hume 1986) and have emissions at variable wavelengths to allow double-labeling strategies. Other advantages of carbocyanines are that 1) they do not transfer from labeled to unlabeled cells (unless membranes are disrupted), 2) their emission wavelengths are independent of tissue pH, and 3) unlike FG, they are not neurotoxic (Naumann et al. 2000).

While the methodological basis for retrograde labeling has been established for decades (Honig and Hume 1986), the labeling of molar teeth and dental primary afferent neurons (DPANs) with crystalline DiI have been described only for rats (Eckert et al. 1997; Kim et al. 2011). In the mouse, molars can hold less dye, and fewer molars can be accessed. Here, we aimed to optimize this technique to enable use in the mouse and permit access to transgenic animal models for functional studies without side effects on physiologic function. We characterized the speed of axonal dye transport to the trigeminal ganglion, the numbers of stained DPANs, and the fluorescence intensity by using conventional crystalline DiI and NeuroTrace, a novel DiI formulation with improved membrane uptake and superior staining efficiency. We describe how to achieve reliable DiI labeling of DPANs in the mouse, and we illustrate our findings with results from cryosections, 2-photon excitation microscopy, and calcium microfluorimetry in live cultures of trigeminal ganglion (TG) neurons.

Methods

Animals

A total of 19 Wistar rats (40 to 81 d) and 14 C57BL/6J mice (61 to 121 d) of both sexes were included in the study. One TRPM8^{EGFP/+} mouse (Dhaka et al. 2008) was used and genotyped as previously described (Vetter et al. 2013). Mice and rats were housed in an in-house open cage facility in a 12-h light-dark cycle according to the European Parliament Council (directive 2007/526/EG). The animal ethics committee and the local district government approved the protocol for in vivo surgical interventions. All experiments were conducted in accordance with the guidelines and regulations of animal care of the European Parliament Council (directive 2010/63EU). The study conforms to the ARRIVE guidelines.

Maxillary Molar Surgery

The anesthesia is induced with sevoflurane (Abbot) and maintained with 90 mg/kg of ketamine (Ketavet; Pharmacia) and 6 mg/kg of xylazine (Rompun 2%; Bayer). Carprofen (4 mg/kg, Rimadyl; Pfizer) and enrofloxacin (7.5 mg/kg, Baytril 5%; Bayer) are applied postoperatively after 12 h and every 24 h for the following 48 to 120 h. The anesthetized animal is in supine position, and the mouth is spread open, with the head kept in position by retractors and eventually rubber bands held by magnetic fixators. Molars are drilled vertically under microscope control until reaching the dentin-pulp border. Pulp bleeding, injury, and contamination of the periodontal tissue must be

avoided. DiI (1,1'-dioctadecyl-3,3,3'-tetramethylindocarbocyanine perchlorate) and NeuroTrace DiI were from Molecular Probes. Molar holes are filled up with the maximal amount of dye and occluded with adhesive and resin-based composite. Both are subsequently applied onto the intact enamel around the cavity and need to be light cured with a halogen 470-nm light source (750 mW/cm²; Translux CL) for 15 and 20 s, respectively. The surgical procedure takes 40 min. An online appendix with extended surgical procedures is available at <http://journals.sagepub.com/home/jdr>.

Collection of TGs

Fourteen mice and 19 rats were euthanized with 50 mg/kg of thiopental and perfused with 4% fresh paraformaldehyde (PFA) in phosphate-buffered saline (PBS) at the respective time points after dye application. Following fixation, the animal was beheaded, the skull opened, and the brain removed. Both TGs were detached from the skull base, with intact branches and dura mater surrounding the ganglia. Ganglia were stored for 4 h in PFA 4% at 4 °C, washed twice for 30 min in PBS, transferred to 30% sucrose in PBS, and stored at 4 °C overnight. The TGs were frozen on dry ice with Tissue-Tek OCT Compound (Sakura) and cut into 14- μ m longitudinal sections with a cryostat (Leica CM3050S; Leica Biosystems). The sections were stained with DAPI and mounted onto poly-L-lysine-coated glass slides with glycerin-free mounting fluid (Fluoromount; Sigma-Aldrich) and cover slips. The sections were micrographed after mounting to prevent dissemination of dye through ruptured membranes.

The immunofluorescent images were acquired with a confocal laser scanning microscope (LSM 710; Carl Zeiss MicroImaging), ZEN 2010 software (Carl Zeiss MicroImaging), and ImageJ 1.48. DiI was examined with a rhodamine filter ($\lambda = 561$ nm), and an FITC filter (493 to 555 nm) was used to recognize lipofuscin autofluorescence and to map the overall structure of the section. Images were taken with a 20 \times objective (0.8 numerical aperture). Images from adjacent sections were compared. The fluorescence level (corrected total cell fluorescence) was calculated with the following formula: integrated density of the selected cell – (area of the selected cell \times mean fluorescence of the background readings).

Parameters were extracted from regions of interest edging labeled cells and background areas.

Two-Photon Microscopy and 3-dimensional Reconstruction

The TRPM8^{EGFP/+} mouse was euthanized by cervical dislocation 5 d postsurgery and decapitated. The skull was opened, the brain removed, and the skull base preparation exposed to 4% PFA overnight. The TG was removed with intact branches and mounted in 1.0% low-melting agarose in a plastic-bottomed culture dish. Image stacks were acquired with a Zeiss LSM 880 NLO equipped with a 680- to 1,300-nm tunable and fixed 1,040-nm 2-photon laser from Newport SpectraPhysics and a

20× W-Plan Apochromat objective lens. Fluorophores were excited at 1,040 nm (DiI) and 920 nm (EGFP [enhanced green fluorescent protein]), and fluorophore emissions were detected with nondescanned GaAsP detectors at 575 to 610 nm (DiI) and 500 to 550 nm (GFP [green fluorescent protein]). **【AQ: 8】** To achieve 3-dimensional reconstruction of the ganglion, 646 Z-slices with 650-nm distance were acquired. Fiji ImageJ was used to process the data and the Cell Counter plug-in for ImageJ to quantify the cells.

Cell Cultures and Calcium Microfluorimetry

Four mice were euthanized by cervical dislocation 5 d postsurgery, and TGs were removed with intact branches. Ganglia were transferred in sterile DMEM (ThermoFisher Scientific) and cut into small pieces. DMEM was subsequently replaced with combined dispase (Gibco; purchased from ThermoFisher Scientific) and collagenase (Sigma-Aldrich) in TNB medium, and the ganglia was incubated at 37 °C and 5% CO₂ for 45 min. The cell suspension was then washed with DMEM and TNB 100 medium, supplemented with TNB 100 lipid-protein complex (Biochrom), 100 µg/mL of streptomycin/penicillin (ThermoFisher Scientific), and 1nM nerve growth factor 7S (Alomone Labs). Cell clusters were triturated in TNB to achieve a cell suspension, and 100 µL of suspension was applied per 1 poly-D-lysine-coated FluoroDish (World Precision Instruments). Dishes were incubated in 1 mL of TNB for 15 to 18 h at 37 °C and 5% CO₂, and after 12 to 18 h in culture, neurons were loaded with Fura-2^{AM} (Invitrogen). Fura-2^{AM} was dissolved in extracellular solution (ECS) containing 145mM NaCl, 5mM KCl, 1mM MgCl₂, 1.25mM CaCl₂, 10mM Hepes, and 10mM glucose; at pH 7.4, the cells were incubated for 30 min and then washed for 15 min in ECS. An automated fast solution changer (CV Scientific) was used to superfuse the cells with ECS, capsaicin (3 µM), and KCl (145 mM). Capsaicin sensitivity was considered for an increase in the calcium response, measured as an area under the curve (AUC) increase >15% over the AUC of the baseline. For baseline and capsaicin response, 120-s time frames were included. The AUC was calculated with the following formula:

$$AUC = \int f(x) dx.$$

In vivo calcium imaging experiments were made with an Olympus IX83 inverted microscope and an Olympus UApoN340 20x water immersion objective. Fura-2^{AM}-loaded cells (3 µm supplemented with 0.02% pluronic dissolved in ECS) were excited with a xenon lamp (Lambda DG-4; Sutter Instrument) at 340 and 380 nm and the emission examined at 510 nm. An ORCA-Flash 4.0 LT digital camera (C11440; Hamamatsu Photonics) was used for image acquisition at a rate of 1/s. DiI was excited at 556 to 590 nm and examined at 602 to 664 nm.

Data Analysis and Statistics

Data in figures are presented as mean ± SEM. Values in text are given as mean ± SD. Unpaired Student's *t* tests and 1-way

analysis of variance were calculated for statistical analysis with Statistica 7.1 (Stat Soft). Differences with *P* values <0.05 were regarded as statistically significant.

Results

Mouse maxillary bone and molars are less than a quarter of the size as those in the rat, and the molars can hold only a fraction of the dye harbored in rat molars. Using crystal DiI in the mouse maxillary molars, we never succeeded in applying sufficient dye quantities to achieve a fluorescence intensity to allow reliable distinction of DPANs from the background. In addition, the third maxillary molar in the mouse is inaccessible. These constraints argue for labeling of fewer mouse DPANs with higher overall intensities. We revisited the rat to evaluate axonal dye diffusion and fluorescence levels to optimize these parameters.

We evaluated the amount of stained DPANs in the trigeminal ganglion after 48, 72, 96, 120, and 168 h of axonal dye transport for DiI crystal and a new DiI gel called NeuroTrace. The average number of labeled neurons in the TG increased, with longer diffusion times for both formulations. Most DPANs were found after 120 h (Fig. 2A): **【AQ: 9】** Crystal DiI stained 44 ± 11 (*n* = 2 ganglia, 2 rats), 62 ± 66 (*n* = 4 ganglia, 3 rats), 49 ± 67 (*n* = 4 ganglia, 2 rats) and 78 ± 34 (*n* = 3 ganglia, 2 rats) after 48, 72, 96, and 120 h, respectively. In contrast, NeuroTrace labeled 18 ± 17 (*n* = 3 ganglia, 3 rats), 19 ± 12 (*n* = 2 ganglia, 1 rat), 19 ± 3 (*n* = 2 ganglia, 2 rats), and 56 ± 14 (*n* = 3 ganglia, 3 rats) after 48, 72, 96, and 120 h, respectively. Using paste, we also assessed after 168 h and found 61 ± 11 DPANs (*n* = 2 ganglia, 2 rats, not illustrated); presumably, 120 h represents the most efficient time frame. Both approaches yielded similar, though not statistically different, results. Nevertheless, staining with NeuroTrace appeared more reliable, as it produced a smaller SD of the sampling distribution (Fig. 1A).

To quantify differences in fluorescence intensity, we assessed corrected total cell fluorescence and found that fluorescence obtained with NeuroTrace was statistically (Fig. 1B) and visibly (Fig. 1C, D) more intense at almost all diffusion times and that it accumulated over time, reaching a peak at 120 h (Fig. 1B).

In the mouse, NeuroTrace successfully stained DPANs, and the average number of neurons increased with time similar to that of the rat (Fig. 2A): NeuroTrace labeled 8 ± 2 (*n* = 4 ganglia, 4 mice), 12 ± 8 (*n* = 2 ganglia, 2 mice) 23 ± 10 (*n* = 5 ganglia, 5 mice) and 31 ± 21 (*n* = 4 ganglia, 3 mice) after 48, 72, 96 and 120 h, respectively. Numbers of labeled DPANs per ganglion ranged between 1 and 52, with 6 ganglia having no labeled DPANs. Because mouse molars contain less fluorescent material, the fluorescence intensity remained lower but sufficient to allow an unambiguous distinction from background (Fig. 2B, C). Size distribution histograms of the cross-sectional area show similar size distributions in rats and mice, and the largest proportion of DPANs were small-diameter nociceptors (Fig. 2D).

Our quantitative assessment of immunofluorescent detection focused on the maxillomandibular area. To study the

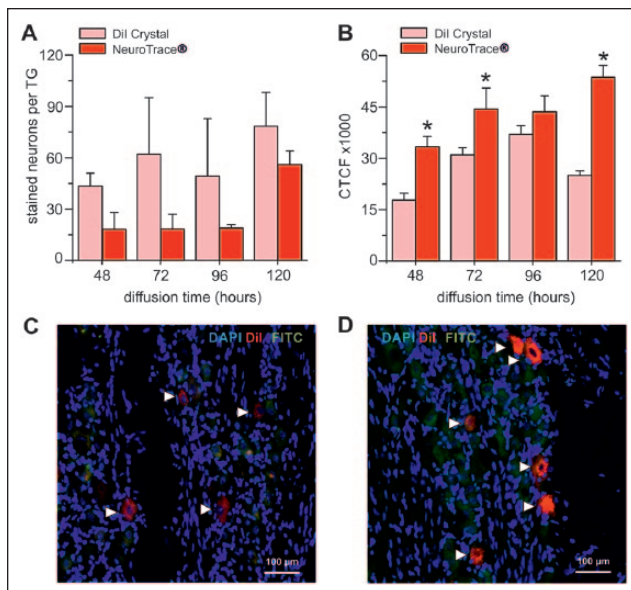


Figure 1. Retrograde labeling characteristics of rat maxillary dental primary afferent neurons (DPANs) with crystalline DiI and NeuroTrace DiI, a new DiI paste composed of an inert water-resistant gel with improved membrane penetration properties. **(A)** Mean \pm SEM number of cells stained per trigeminal ganglion (TG) as a function of the DiI diffusion time (23 ganglia were included from 19 rats). Dye diffusion time of 5 d provided the highest amount of fluorescent cells in ganglia for both crystal and paste. The reproducibility was superior with the paste, resulting in a smaller SEM. **(B)** Fluorescence intensity of labeled trigeminal neurons as a function of the DiI diffusion time for paste (red) and crystal (light red). The fluorescence intensity was determined as corrected total cell fluorescence (CTCF) and calculated as described in Methods. NeuroTrace DiI paste stained the neurons with a higher fluorescence intensity, which resulted in a better distinction from background than crystal dye at nearly all time points ($^{*}P < 0.05$, *t* test). **(C, D)** Confocal photomicrographs of cryosections of TG with DPANs labeled with **(C)** crystal or **(D)** NeuroTrace DiI tissue-labeling paste (labeled cells marked with arrowheads).

spatial distribution of maxillary DPANs, we reconstructed an entire mouse TG from image stacks obtained with a 2-photon microscope. Figure 3 illustrates DPANs in a TRPM8^{EGFP/+} TG. We identified a total of 176 DPANs and mapped the distribution in the 3 subregions of the TG. Briefly, more than half of the DPANs ($n = 100$, 57%) are located in V3, the mandibular division; 38% ($n = 67$) are contained in V2, the maxillary division; and the remaining 5% ($n = 9$) are spread throughout the ophthalmic division. Remarkably, the largest cluster of DPANs is aggregated in the anterior part of the mandibular division, and it contains the majority—that is, two-thirds of the TRPM8-containing DPANs (Fig. 3D, E).

Last but not least, we tested whether the staining of mouse DPANs with DiI was also appropriate for functional assessment, using *in vivo* calcium imaging with the ratiometric calcium dye Fura-2^{AM}. In dissociated TG cultures, fluorescent DPANs were well discernable (Fig. 4A–C). DiI-labeled cells were subjected to simulation with 3 μ M capsaicin in ECS. Subsequently, high-potassium solution was applied to differentiate neurons from glia (Fig. 4D). The increase in intracellular

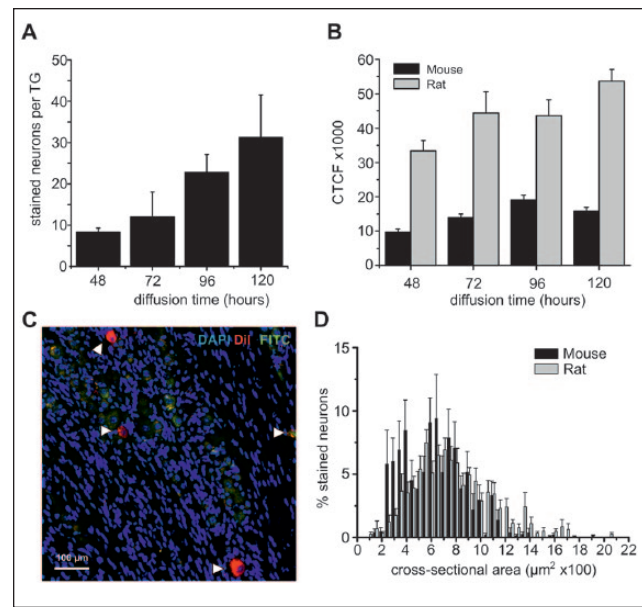


Figure 2. Retrograde labeling of mouse maxillary dental primary afferent neurons (DPANs) with NeuroTrace DiI paste. **(A)** The mean \pm SEM number of cells stained per trigeminal ganglion (TG) as a function of the DiI diffusion time (15 ganglia were included from 14 mice) is lower in the mouse because only 2 instead of 3 molars can be accessed for labeling. **(B)** The fluorescence intensity is significantly lower in mouse DPANs as compared with the rat, irrespective of the diffusion time ($^{*}P < 0.01$, *t* test) because the mouse molars contain less fluorescent material. The fluorescence intensity was determined as corrected total cell fluorescence (CTCF) and calculated as described in Methods. **(C)** Confocal photomicrograph of a cryosection of a mouse TG with DPANs stained with NeuroTrace DiI tissue-labeling paste (arrowheads). **(D)** Size distribution of labeled DPANs in bins per 50 μ m² and determined as cross-sectional area for mouse (black) and rat (red). Tooth pulp afferents are a highly enriched population of small diameter nociceptors.

calcium of the DPANs was not different from the nonlabeled adjacent neurons (Fig. 4E; $P = 0.4$, *t* test)

Discussion

Retrograde labeling of tooth pulp afferents is a key method to investigate the properties of tooth nociceptors. Yet, this method has been predominantly used in the rat through crystal DiI (Taddese et al. 1995; Eckert et al. 1997; Chaudhary et al. 2001; Park et al. 2006; Kim et al. 2011; Vang et al. 2012). In the mouse, so far only FG was employed successfully and applied with pulp access to the 2 front maxillary molars (Lin et al. 2015) or to the dentinal surface of 1 molar (Chung et al. 2011, 2012). In contrast to the carbocyanine dyes (Honig and Hume 1989), FG is neurotoxic (Naumann et al. 2000), but it outmatches DiI in its brighter and longer-lasting fluorescence and its greater uptake by axonal membranes (Schmued and Fallon 1986), which makes it similar to NeuroTrace and may explain why both, in contrast to crystal DiI, allowed successful mouse DPAN staining despite the anatomic limitations.

An unexpected finding was the occurrence of the majority of maxillary molar DPANs in the mandibular and also, to a

minor extent, the ophthalmic parts of the reconstructed TG. One earlier study utilized horseradish peroxidase (HRP) deposited in cat canine dental pulp, and it found that innervating neurons were indeed occasionally located in the mandibular and ophthalmic areas (Anderson and Rosing 1977); yet, another study described separate locations for cell bodies innervating lower and upper cat canines in the mandibular and maxillary divisions (Arvidsson 1975). For cat and monkey, a somatotopic organization of the trigeminal ganglion, foremost for tactile information, is in good agreement with earlier physiologic and anatomic studies (Kerr and Lysak 1964; Beaudreau and Jerge 1968; Lende and Poulos 1970). For the rat, chromatolytic changes following trigeminal nerve branch transection showed that dental afferent innervation follows a predominant medio-lateral but no dorsoventral somatotopic pattern (Mazza and Dixon 1972; Gregg and Dixon 1973). Our large cluster of DPANs identified in the anterior part of the mandibular division, with some continuation in the maxillary division, is in accordance with this finding. Although species differences may account for a progressive reduction of somatotopy in rodents, the concept of vertebrate jaw development provides an additional convincing explanation for the distribution of the DPANs. In the craniofacial developmental program, the upper jaw develops as a composite structure, and the ophthalmic nerve is not segregated (Higashiyama and Kuratani 2014). The rostral part of the upper jaw is derived from the premandibular domain, which receives innervation from ophthalmic nerve branches, while the posterior part arises from the mandibular arch, innervated by the maxillomandibular component (Higashiyama and Kuratani 2014).

Immunohistochemistry yielded a large variability of DPAN cell counts among individual experiments but also in comparison with the 3-dimensional reconstruction. Technical shortcomings—including inhomogeneous distribution of different dye quantities and, hypothetically, some leak through the root apical foramen—may contribute to the observation; previous labeling studies based on HRP transport also saw substantial variation in DPAN counts, but this concerned the overall amount of cells harbored in 1 TG, which is why these are most likely highly individual parameters. In 2 studies, the total cell number of 1 rat TG ranged between 23,258 and 46,713 (Aldskogius and Arvidsson 1978) and 40,910 to 62,030 (Gregg and Dixon 1973); in the latter study, cell bodies associated with maxillary or mandibular molar innervation accounted for ~1% of TG cells, as quantified by chromatolysis after root apex transection (Gregg and Dixon 1973). Comparable with our experiments—in which we observed a 50% failure rate (i.e., 14 mice with labeled DPANs in at least 1 ganglion were included,

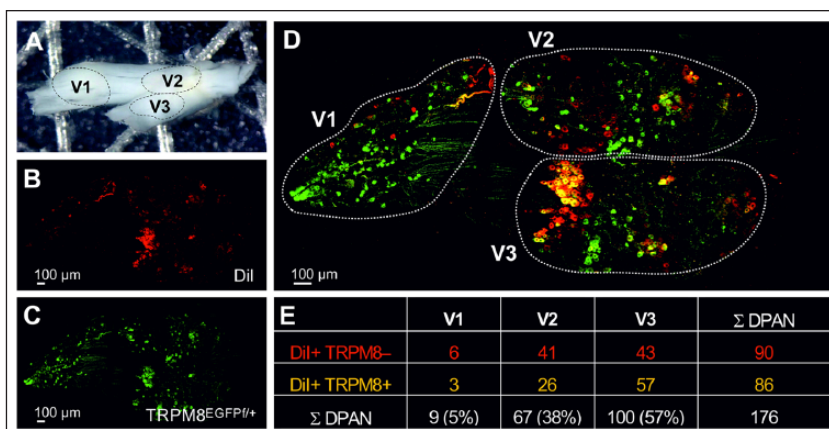


Figure 3. Spatial distribution of the dental primary afferent neurons (DPANs) of the first 2 maxillary molars in the 3 sections of the trigeminal ganglion of a TRPM8^{EGFP/+} mouse. The DPANs were visualized from a 3-dimensional reconstruction of image stacks obtained with a 2-photon laser scanning microscope. (A) Transmitted light photomicrograph of the trigeminal ganglion highlighting the ophthalmic (V1), maxillary (V2), and mandibular (V3) sections. (B–D) Two-photon laser scanning microscope images of the trigeminal ganglion showing the retrograde-labeled DPANs in red (B), TRPM8 in farnesylated enhanced green fluorescent protein (EGFP; C), and a merged view of both images (D). The sections were identified following (Boada 2013). (E) Quantification of DPANs with and without TRPM8 in 3 sections of trigeminal ganglion. An online appendix with a 3-dimensional view is available at <http://journals.sagepub.com/home/jdr>.

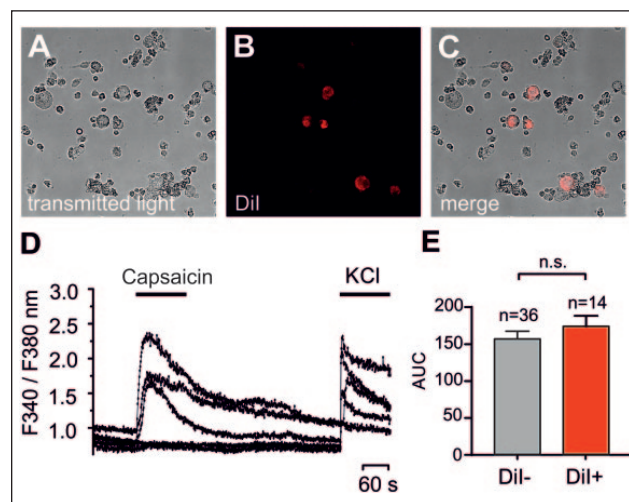


Figure 4. Capsaicin sensitivity of mouse Dil-labeled maxillary dental primary afferent neurons (DPANs) in TG cultures. (A–C) Photomicrographs of mouse TG neurons in cell culture with Dil in red discerning the DPANs. (D) Representative calcium transient of capsaicin-sensitive and capsaicin-insensitive (3 μM) DPANs depicted as ratio. Potassium chloride (KCl, 145 mM) was applied to identify neurons. (E) The increase in intracellular calcium in response to capsaicin (3 μM) is not different in presence or absence of Dil. Data are from 4 male C57BL/6J mice, and ganglia from 2 mice were used for each culture. Values are presented as mean ± SEM.

but in another 14 animals, the surgery yielded no labeled DPANs—a work with HRP in the cat reported a rate of 30% failed experiments, with no labeling after HRP exposure (Arvidsson 1975). Nevertheless, with the high level of manual and technical skills required for this particular surgery in the mouse, we consider a 50% success rate a reproducible approach

for DPAN visualization, especially because the number of dropouts decreased noticeably with practice and experience. In this study, the number of cells with HRP granula was between 5 and 136 per tooth—quite similar to the variability in our hands. Another HRP study estimated 163 cells to innervate 1 feline canine tooth (Anderson and Rosing 1977) and a third one, as much as 199 cells (Pearl et al. 1977). Two previous studies with DiI in the rat found that 1) 30 to 50 DPANs are labeled, albeit counted in dissociated TG cultures and after crystal DiI exposure of all maxillary molar pulps (Taddese et al. 1995; Eckert et al. 1997) and 2) about 136 ± 58 were counted from immunohistochemical analysis in the rat following HRP labeling (Sugimoto et al. 1988). In a further study, where 1 rat mandibular molar was exposed to HRP, the counted cells ranged from 142 to 288 (Aker 1987). Our 2-photon reconstruction, which we regard as the most accurate method to date, identified 176 DPANs from 2 mouse maxillary molars.

Our model is appropriate for morphologic studies using immunohistochemistry and functional studies of single cultured neurons, such as patch clamp, calcium microfluorimetry, and polymerase chain reaction (Taddese et al. 1995; Cook et al. 1997; Chung et al. 2011; Kim et al. 2011; Vang et al. 2012). The model does rely on the fact that only dental primary afferents appear labeled. Although the tooth constitutes a natural barrier, dye leakage and dissemination via the root or disintegrated mucosal and periodontal tissue represent a realistic concern, and the periodontal ligament in particular has abundant sensory innervation (Arvidsson 1975). In our hands, application of dye to bleeding pulp resulted in few or no labeled cells; similarly, application to uninjured pharyngeal mucosa yielded no staining. Under microscope control, dye leakage and injury to the adjacent periodontal ligament/tissue can be excluded. Our control experiments are supported by previous findings that DiI in the bloodstream does not contribute to labeling and that only axons with disintegrated membrane serve to dye uptake (Eckert et al. 1997). Nevertheless, a dissemination of dye through the root apical foramen into periodontal tissue cannot be controlled for but should matter only in case of injury; even then, it is highly likely that uptake of the dye in dental pulp and root nerves occurs in these cases as well.

In rats, DiI labeling allowed patch clamp recordings and led to recognition of the majority of dental primary afferents as nociceptors with capsaicin sensitivity and a characteristic hump in the action potential shape (Kim et al. 2011). Immunofluorescence identified nociceptors as IB4 binding and verified expression of TRPV1 and specific ligand-gated ion channels for ATP (P2X₂, P2X₃). Based on reverse transcription polymerase chain reaction, TRPM8, TRPA1, and the nociceptor-specific sodium channel subtype Na_v1.8 (Cook et al. 1997; Kim et al. 2011; Vang et al. 2012) were detected. In our reconstruction from a C57BL/6J mouse, we found that 49% of the DPANs expressed TRPM8. In contrast, in rat TGs, single-cell reverse transcription polymerase chain reaction identified mRNA from TRPM8 in 35% of the DPANs. The difference may be due to alterations under culture conditions or may be species dependent (Kim et al. 2011). Mainly nociceptors and

only a few A β -like DPANs were identified by staining with the neurofilament 200 marker in the rat (Vang et al. 2012), which also matches the size distribution histogram established in our study for both species.

In summary, our study provides first-time evidence that specific retrograde labeling from mouse dental afferents is possible with carbocyanine dyes. We regard the possibility of retrograde labeling of dental afferents in mice as an enabling technology. In particular, future studies can now combine the strength of transgenic mouse models and single-cell transcriptomics with morphology and functional characterization of neuronal subpopulations. Such integrative studies are necessary to recognize the mechanistic basis of how tooth pain segregates from trigeminal, somatic, and visceral pain and to support the development of therapeutic approaches for dentine hypersensitivity and tooth pain.

Author Contributions

A. Kadala, P. Sotelo-Hitschfeld, contributed to conception, design, data acquisition, analysis, and interpretation, drafted and critically revised the manuscript; Z. Ahmad, A. Mueller, L. Bernal, Z. Winter, contributed to data acquisition, critically revised the manuscript; P. Tripal, B. Schmid, contributed to conception, design, data acquisition, and analysis, critically revised the manuscript; S. Brauchi, contributed to data interpretation, critically revised the manuscript; U. Lohbauer, contributed to conception and design, critically revised the manuscript; K. Messlinger, J. Lennerz, contributed to conception, design, and data interpretation, critically revised the manuscript; K. Zimmermann, contributed to conception, design, data analysis, and interpretation, drafted and critically revised the manuscript. All authors gave final approval and agree to be accountable for all aspects of the work.

Acknowledgments

Part of the present work was performed in fulfillment of the requirements for obtaining the degree dentariae medicinae doctoris (Dr med dent). The authors thank Birgit Vogler and Jana Schramm for expert technical assistance. This study was funded by IZKF Project E14, the Pfleger Foundation, and the German Research Council (DFG ZI 1172/3-1 and ZI 1172/4-1). P.S.H. acknowledges support from CONICYT (21140372) and MECESUP (AUS 1203) fellowships. The authors declare no potential conflicts of interest with respect to the authorship and/or publication of this article. **[AQ: 10]**

References

- Aker FD. 1987. Innervation of rat molar teeth: II. A quantitative analysis of primary sensory neurons innervating a mandibular molar tooth. *Anat Rec*. 219(2):186–192.
- Aldskogius H, Arvidsson J. 1978. Nerve cell degeneration and death in the trigeminal ganglion of the adult rat following peripheral nerve transection. *J Neurocytol*. 7(2):229–250.
- Anderson KV, Rosing HS. 1977. Location of feline trigeminal ganglion cells innervating maxillary canine teeth: a horseradish peroxidase analysis. *Exp Neurol*. 57(1):302–306.

- Arvidsson J. 1975. Location of cat trigeminal ganglion cells innervating dental pulp of upper and lower canines studied by retrograde transport of horseradish peroxidase. *Brain Res.* 99(1):135–139.
- Beaudreau DE, Jerge CR. 1968. Somatotopic representation in the gasserian ganglion of tactile peripheral fields in the cat. *Arch Oral Biol.* 13(3):247–256.
- Boada MD. 2013. Relationship between electrophysiological signature and defined sensory modality of trigeminal ganglion neurons in vivo. *J Neurophysiol.* 109(3):749–757.
- Chaudhary P, Martenson ME, Baumann TK. 2001. Vanilloid receptor expression and capsaicin excitation of rat dental primary afferent neurons. *J Dent Res.* 80(6):1518–1523.
- Chung MK, Jue SS, Dong X. 2012. Projection of non-peptidergic afferents to mouse tooth pulp. *J Dent Res.* 91(8):777–782.
- Chung MK, Lee J, Duraes G, Ro JY. 2011. Lipopolysaccharide-induced pulpitis up-regulates TRPV1 in trigeminal ganglia. *J Dent Res.* 90(9):1103–1107.
- Cook SP, Vulchanova L, Hargreaves KM, Elde R, McCleskey EW. 1997. Distinct ATP receptors on pain-sensing and stretch-sensing neurons. *Nature.* 387(6632):505–508.
- Dhaka A, Earley TJ, Watson J, Patapoutian A. 2008. Visualizing cold spots: TRPM8-expressing sensory neurons and their projections. *J Neurosci.* 28(3):566–575.
- Eckert SP, Taddese A, McCleskey EW. 1997. Isolation and culture of rat sensory neurons having distinct sensory modalities. *J Neurosci Methods.* 77(2):183–190.
- Gregg JM, Dixon AD. 1973. Somatotopic organization of the trigeminal ganglion in the rat. *Arch Oral Biol.* 18(4):487–498.
- Higashiyama H, Kuratani S. 2014. On the maxillary nerve. *J Morphol.* 275(1):17–38.
- Honig MG, Hume RI. 1986. Fluorescent carbocyanine dyes allow living neurons of identified origin to be studied in long-term cultures. *J Cell Biol.* 103(1):171–187.
- Honig MG, Hume RI. 1989. Dil and diO: versatile fluorescent dyes for neuronal labelling and pathway tracing. *Trends Neurosci.* 12(9):333–335, 340–341.
- Kerr FW, Lysak WR. 1964. Somatotopic organization of trigeminal-ganglion neurones. *Arch Neurol.* 11:593–602.
- Kim HY, Chung G, Jo HJ, Kim YS, Bae YC, Jung SJ, Kim JS, Oh SB. 2011. Characterization of dental nociceptive neurons. *J Dent Res.* 90(6):771–776.
- Lende RA, Poulos DA. 1970. Functional localization in the trigeminal ganglion in the monkey. *J Neurosurg.* 32(3):336–343.
- Lin JJ, Du Y, Cai WK, Kuang R, Chang T, Zhang Z, Yang YX, Sun C, Li ZY, Kuang F. 2015. Toll-like receptor 4 signaling in neurons of trigeminal ganglion contributes to nociception induced by acute pulpitis in rats. *Sci Rep.* 5:12549.
- Mazza JP, Dixon AD. 1972. A histological study of chromatolytic cell groups in the trigeminal ganglion of the rat. *Arch Oral Biol.* 17(3):377–387.
- Naumann T, Hartig W, Frotscher M. 2000. Retrograde tracing with Fluoro-Gold: different methods of tracer detection at the ultrastructural level and neurodegenerative changes of back-filled neurons in long-term studies. *J Neurosci Methods.* 103(1):11–21.
- Park CK, Kim MS, Fang Z, Li HY, Jung SJ, Choi SY, Lee SJ, Park K, Kim JS, Oh SB. 2006. Functional expression of thermo-transient receptor potential channels in dental primary afferent neurons: implication for tooth pain. *J Biol Chem.* 281(25):17304–17311.
- Pearl GS, Anderson KV, Rosing HS. 1977. Anatomic evidence revealing extensive transmedian innervation of feline canine teeth. *Exp Neurol.* 54(3):432–443.
- Schmued LC, Fallon JH. 1986. Fluoro-Gold: a new fluorescent retrograde axonal tracer with numerous unique properties. *Brain Res.* 377(1):147–154.
- Sugimoto T, Takemura M, Wakisaka S. 1988. Cell size analysis of primary neurons innervating the cornea and tooth pulp of the rat. *Pain.* 32(3):375–381.
- Taddese A, Nah SY, McCleskey EW. 1995. Selective opioid inhibition of small nociceptive neurons. *Science.* 270(5240):1366–1369.
- Usoskin D, Furlan A, Islam S, Abdo H, Lonnerberg P, Lou D, Hjerling-Leffler J, Haeggstrom J, Kharchenko O, Kharchenko PV, et al. 2015. Unbiased classification of sensory neuron types by large-scale single-cell RNA sequencing. *Nat Neurosci.* 18(1):145–153.
- Vang H, Chung G, Kim HY, Park SB, Jung SJ, Kim JS, Oh SB. 2012. Neurochemical properties of dental primary afferent neurons. *Exp Neurobiol.* 21(2):68–74.
- Vetter I, Hein A, Sattler S, Hessler S, Touska F, Bressan E, Parra A, Hager U, Leffler A, Boukalova S, et al. 2013. Amplified cold transduction in native nociceptors by M-channel inhibition. *J Neurosci.* 33(42):16627–16641.